

VERY LOW OUTPUT IMPEDANCE RF SYSTEM FOR HIGH INTENSITY ACCELERATORS

Y. Irie

KEK National Laboratory for High Energy Physics
Oho 1-1, Tsukuba-shi, Ibaraki-ken, 305 Japan

abstract : A model RF system with a cathode follower was tested under frequency modulation in the 1-3.5 MHz range. The repetition rate was 40 Hz. The oscillation was stable, and no liability to parasitic oscillations has been observed. An energy problem associated with this scheme is also mentioned.

1. Introduction

The cathode follower RF system was first implemented as a beam buncher in the Proton Storage Ring at the Los Alamos National Laboratory.¹⁾ For further applications to synchrotrons, it is necessary to study the feasibility under frequency modulation. A model RF system with a cathode follower²⁾ is being tested for this purpose. This report describes the results of the preliminary tests.

2. Stability analysis

The cathode follower is inherently liable to spurious oscillations when the cathode load is capacitively tuned (Fig.1). If the grid current (i_g) is negligible compared to the other branch currents, the cathode voltage (e_k) is given by

$$e_k = \frac{\mu}{\mu + 1} e_{in} \frac{Z_k}{r/(\mu + 1) + Z_k},$$

where Z_k is the cathode load, μ the amplification factor, r the plate resistance and the beam is assumed to be absent for the moment. Since $-i_g = j \omega C_g (e_k - e_{in})$, where C_g is the cathode-grid capacitance, the scalar product of e_{in} and $-i_g$ is negative for an inductive load and is positive for a capacitive load (Fig.2). The energy is then fed back to the driver stage through C_g for the latter case and the system possibly becomes unstable. Since this phenomenon is transient, a stability criterion should be used for the analysis.

Suppose that the driver stage comprises a tank circuit (L_d, C_d), and the cathode load an RF cavity with beam current (i_b). The driver voltage with an initial charge Q_0 in C_d is then written as

$$e_{in} = Q_0 \frac{s^3 (C + C_g) L_d r + s^2 (\mu + 1 + r/R) L_d + s \omega_0^2 C L_d r}{a_0 s^4 + a_1 s^3 + a_2 s^2 + a_3 s + a_4} - \frac{I_1 s + I_2 \omega}{s^2 + \omega^2} \frac{s^3 C_g L_d r}{a_0 s^4 + a_1 s^3 + a_2 s^2 + a_3 s + a_4},$$

where $i_b = (I_1 s + I_2 \omega) / (s^2 + \omega^2)$, ω_0 is the cavity resonant frequency $(\sqrt{LC})^{-1}$, R is the shunt resistance, and the coefficients in the denominator are:

$$\begin{aligned}
a_0 &= [C_d C_g + C (C_d + C_g)] L_d r, \\
a_1 &= C_g L_d + (\mu + 1) C_d L_d + (C_d + C_g) L_d r / R, \\
a_2 &= [C + C_g + \omega_0^2 C (C_d + C_g) L_d] r, \\
a_3 &= \mu + 1 + r / R,
\end{aligned} \tag{1}$$

and

$$a_4 = \omega_0^2 C r.$$

It is interesting that no beam component appears in eq.(1), ie the beam loading has no influence upon whether or not the pole has a positive real component. According to the Hurwitz criterion, the following terms should have positive sign for stable operation:

$$b_1 \approx \omega_0^2 C C_d L_d r > 0$$

and

$$c_1 \approx \frac{\mu C_g (\omega_0^2 C_d L_d - 1)}{\omega_0^2 C_d^2 L_d} \tag{2}$$

where we have assumed that C_g is small compared to C and C_d . Corresponding to the difference in the resonant frequency between the driver circuit and the cathode load, c_1 changes sign. For a capacitive load, it is negative and the system becomes unstable, which is consistent with the discussion above. Hence, it seems that cavity tuning control is effective for stable RF operation.

3. RF system

Figure 3 shows the system setup. Two cavities are connected by a single-turn bias winding, either of which is directly coupled to the cathode of the final amplifier. Five ferrite rings with cooling plates are stacked in each cavity. A 30-ohm resistor is installed at the grid input of the cathode follower to prevent the likelihood of vigorous oscillations. In the driver stage high power tetrode (max. plate dissipation 90 kw) was used to drive a 500-ohm resistor across the grid input. Table 1 summarises the parameters.

The bias power supply for cavity ferrites comprises a dc plus a resonant power source, which was originally purchased to study a ring magnet power supply at a high repetition rate. The output current has a shape of the dc-biased sinusoidal wave at a 40 Hz repetition. The power supply has just been provided with a self-trigger system to maintain the oscillation at resonance. Since the ac amplitude was limited to 250 A, the bias current was divided into three groups (200-700 A, 700-1200 A and 1200-1700 A) to cover the entire range of the RF frequency of interest.

A Tektronix programmable arbitrary/function generator produces a predetermined reference voltage for a voltage-controlled oscillator (VCO) at a constant clock rate. The waveform is generated with 12-bit resolution and the full scale of memory is 8192 points. The start of the generator cycle is synchronized with the repetition of the bias power supply. The phase difference between the grid voltage and the cathode current, the sensor of which is a Pearson model 150 current transformer, is also fed into the VCO. The level control loop is incorporated only to keep the preamplifier output constant.

4. Output impedance and high power results

A Hewlett Packard 4195A network analyser was used to measure the output impedance; the probe was connected to the 'cold' gap where no quiescent current flows. Figure 4 shows a typical result compared with calculations using an electronic circuit simulation program, Spice. In the

calculation, $\mu = 18$, $r = 370$ ohm, $C_g = 70$ pF and any stray capacitances (C_{stray}) across the grid input were estimated to be 83 pF. The bias current for ferrites was adjusted to the resonance at 2.5 MHz. The peak at 4.5 MHz showed a parasitic resonance through the inductance ($0.3 \mu\text{H}$) of the bias winding loop, where the gap voltages of the two cavities swung 180° out-of-phase with nearly the same amplitudes.²⁾ The calculation also fits the other spikes and the steep slope at higher frequencies, where contributions are from the lead inductance of the measuring probe and the cavity capacitors, as well as the bypass capacitor at the feeding point of the cavity bias current. The output impedance seen by the beam is summarised in Fig. 5. Inadequate grounding of the anode circuit is thought to be a reason for the large amplitude near 1 MHz. A slight increase of the impedance with frequency is due to the fact that less voltage is developed between the grid and the cathode as the frequency becomes higher; hence, the characteristic of low output impedance will be diminished. To make the calculation independent of the cavities, we directly look into the cathode and the cathode-grid reactance in series with whatever appears between grid and ground in the driver stage (Fig.1). The impedance thus seen gives $r/(\mu+1)$ at a lower frequency, and increases with frequency. The results for the present system are $20 \text{ ohm} \angle 5^\circ$ at 500 kHz and $33 \text{ ohm} \angle -16^\circ$ at 50 MHz. These values are still low.

The same resonances can be seen for the grid input impedance. Figure 6 shows the result of a Spice calculation, in which the cavity inductance is taken to be same as in Fig.4. In the figure, the dashed line indicates the approximate impedance of a 500-ohm resistor in parallel with the total capacitance across the grid input. The total capacitance (C_{gg}) is given as

$$C_{gg} = C_{stray} + C_g (1 - A),$$

where A is the voltage gain of the cathode follower.³⁾ However, the second term in the right-hand side was approximated by C_g in the calculation, which is really the case except for the resonance region.

Figure 7 displays RF wave forms over the range of 1.1-2.3 MHz. The voltages are lower by half or less than expected from the low-level measurements of the cavity shunt impedance.²⁾ The preliminary result for an RF voltage is at most 500 V per two gaps at 1.2 MHz. However, the oscillation was stable and no liability to parasitic oscillations has been observed. In order to see the effect of cavity tuning as discussed in section 1, a test was also made under fixed frequencies, which were slightly shifted from the resonance. However, contrary to eq.(2) the result indicated no buildup of oscillations.

5. Discussions

It seems worthwhile at this point to mention the power consumption at the driver stage,⁴⁾ since the voltage gain of the cathode follower is less than unity. At higher frequencies, the reactance due to the total capacitance between the grid and ground becomes a dominant term (Fig.6), and a much higher current will be required than that of the final stage amplifier. The cathode follower should be therefore used far below the frequency $\mu/(2\pi r C_{gg})$, where the output impedance is equal to the driver-stage reactance. The choice of cathode follower to high intensity accelerators depends upon the beam loading and necessary RF voltage.

Acknowledgments

The author would like to express his gratitude to Messrs Y. Yano, N. Kaneko and Y. Kobayashi for their cooperation.

References:

- 1) T. Hardek: Preprint LA-UR-84-1935.
- 2) Y. Irie, N. Kaneko, H. Baba and M. Miki: KEK Report 87-28, 1988.
- 3) F. Clapp: Proc. I.R.E., 37, (1949) pp.932-937.

Table1. Parameters of the cathode follower RF system

Repetition frequency	40	Hz
RF frequency	1-4	MHz
Cavity		
Inductance	2.4-0.15	μH
Resonating capacitance	10.5	nF
Ferrite material	TDK SY-5	
inner radius	0.12	m
outer radius	0.22	m
thickness	0.025	m
No. of ferrite rings / cavity	5	
Bias loop	1	turn
Bias current	200-1700	ampere
Final Amplifier		
Class of operation	A	
Type	Cathode follower	
Configuration	single-ended	
Power tube	Eimac 3CW40,000H3	
Driver Amplifier		
Class of operation	A	
Type	Grounded cathode	
Power tube	Ziemens RS2058CJ	

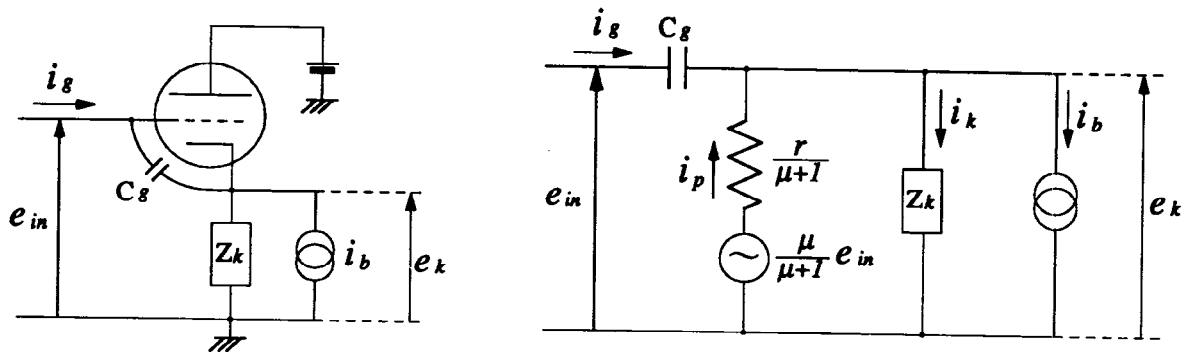


Fig.1 Cathode follower and its equivalent circuit.

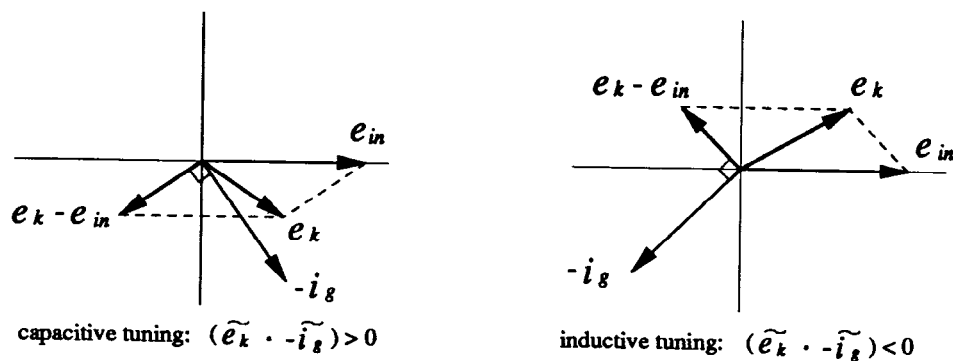


Fig.2 Phasor diagram for the cathode follower.

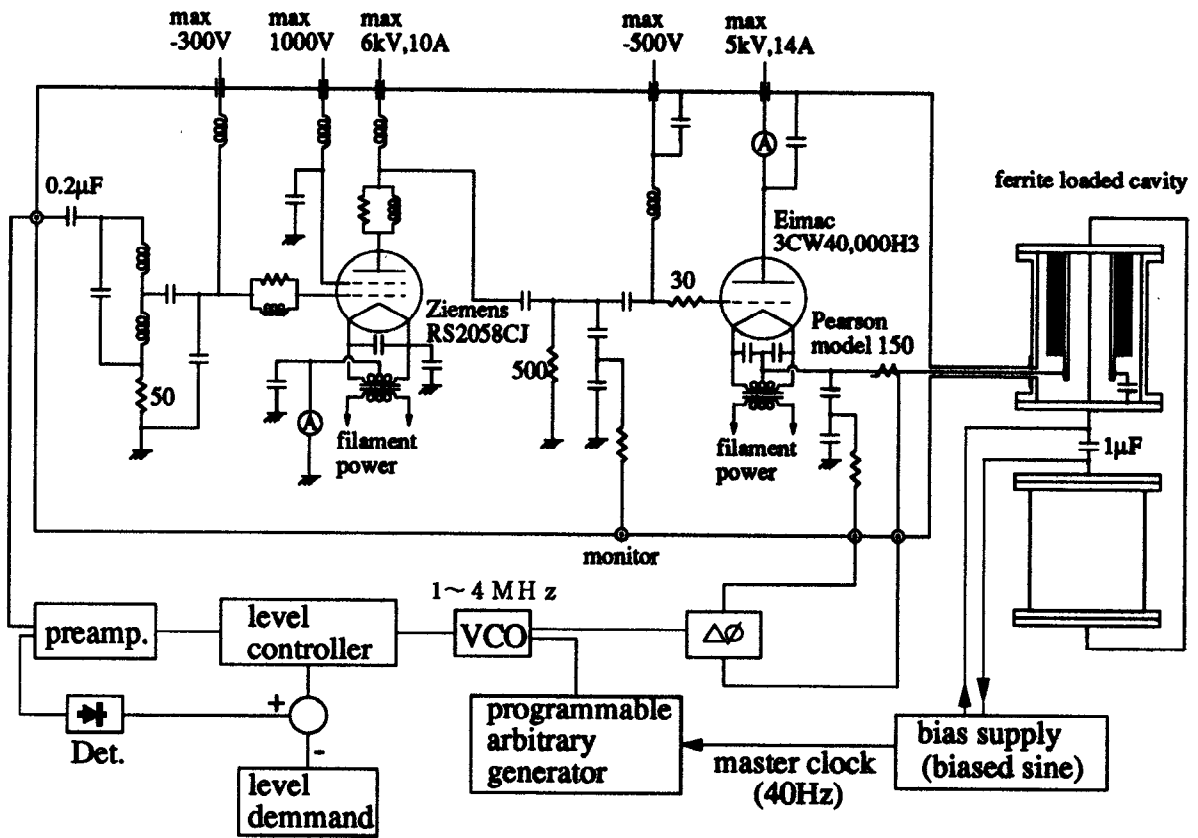


Fig.3 Setup of the RF system.

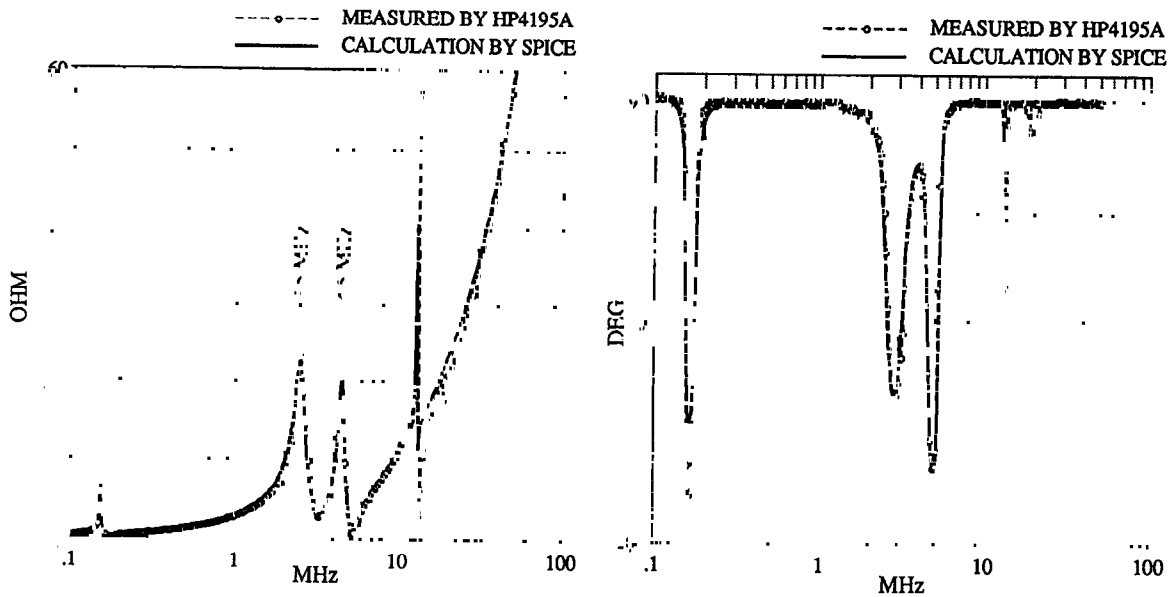


Fig.4 Typical result of an output impedance measurement.

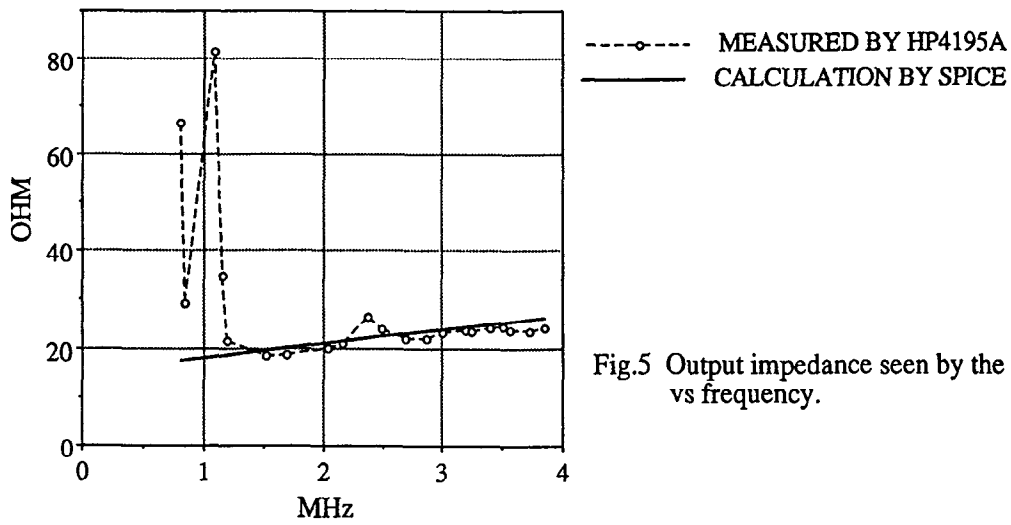


Fig.5 Output impedance seen by the beam vs frequency.

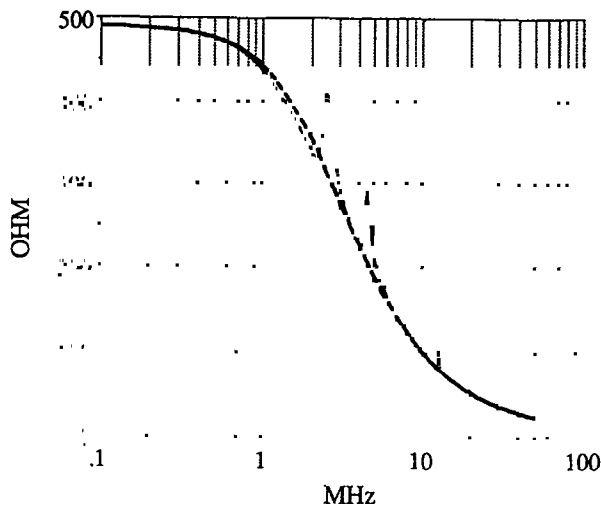


Fig.6 Grid input impedance (solid) and approximation by $C_g(1-A) \sim C_g$ (dashed).

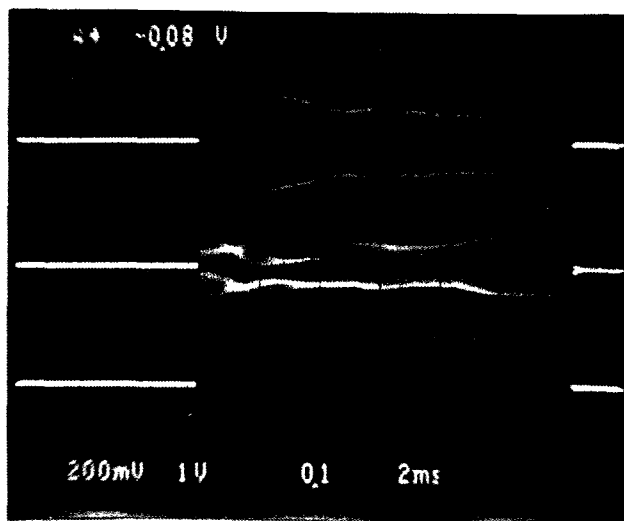


Fig. 7
From the upper to the lower traces:
the grid input voltage (200 V/div),
cavity input current (2 A/div), and
cathode voltage (100 V/div)
over the range of 1.1-2.3 MHz.